Biology of Reproduction, 2025, **112(6)**, 1134–1147
https://doi.org/10.1093/biolre/ioaf062
Advance access publication date 26 March 2025
Research Article

The roles of AKT isoforms in decidualization and embryo implantation using a Progesterone Receptor-Cre mouse model†

Pascal Adam[1], François Fabi[2], Sophie Parent[1], Léa-Isabelle Renaud[1], Monique Cadrin[1] and Eric Asselin[1,*]

[1]Département de Biologie Médicale, Université du Québec à Trois-Rivières, Trois-Rivières, Québec, Canada
[2]Service de radio-oncologie du Département de médecine spécialisée, Centre intégré de cancérologie, Hôpital de l'Enfant-Jésus, Centre Hospitalier Universitaire (CHU) de Québec—Université Laval, Québec, Canada

***Correspondence:** Département de Biologie Médicale, Université du Québec à Trois-Rivières, C.P. 500, 3351 blvd des Forges, Trois-Rivières, Québec G8Z 4M3, Canada. E-mail: eric.asselin@uqtr.ca

†**Grant Support:** This work was supported by the Natural Sciences and Engineering Research Council of Canada (NSERC) (RGPIN 2019-06151).

Abstract

Implantation is a complex process requiring a prepared, receptive endometrium, reliant on synchronized decidualization of stromal cells. During this process, cell proliferation and apoptosis are tightly regulated by signaling factors, including the survival and proliferation of the PI3K/AKT pathway. The three AKT isoforms each play distinct physiological roles, but their specific functions in endometrial cell survival and apoptosis remain unclear. We hypothesize that for successful implantation, each AKT isoform has distinct roles in the endometrium during decidualization, which varies throughout the process. To explore this, we developed a unique PGR-Cre tissue-specific mouse model with single and combined knockouts (KO) of each AKT isoform. Using artificial decidualization during pseudopregnancy and normal gestation, we investigated the specific activity of each AKT isoform and their downstream targets to assess the role of AKT pathway. Our results showed that the AKT1–2 KO genotype failed to decidualize during pseudopregnancy and exhibited a reduced number of implantation sites. Interestingly, AKT3 was hyperphosphorylated in the AKT1–2 KO mice and emerged as the primary isoform active throughout decidualization, specifically signaling through GSK3B. This study suggests distinct yet partially redundant roles for AKT1 and AKT2 during decidualization and embryo implantation. We propose that the AKT pathway plays significant role in fertility, and a deeper understanding of its involvement in decidualization could lead to improved strategies for addressing fertility issues. These findings highlight the importance of AKT activity in the cellular and molecular regulation of mouse fertility.

Graphical Abstract

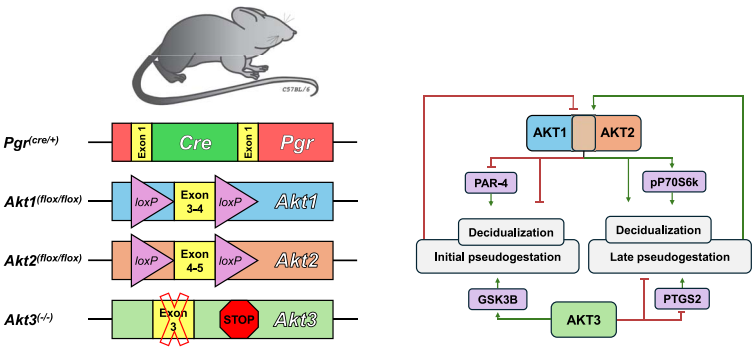

Key words: AKT isoforms, decidualization, pseudogestation, implantation, PGR-Cre knockout, mouse, fertility

Introduction

Infertility has become a growing concern throughout the developed world [1]. A 2012 study showed that 16% of Canadian couples have difficulties conceiving, a figure that has doubled over the last 30 years [2]. Partly due to the rise in infertility and subfertility rates, up to 4% of births in Canada are now conceived using some form of infertility treatment [3]. It is a complex condition with a multitude of contributing factors, encompassing a wide range of diseases, physiological abnormalities, and pathological phenomena [4–6]. Despite this diversity of causes, a common thread in many cases of infertility is the failure of effective communication between the embryo and the maternal endometrium [7, 8]. This intricate communication process is essential for a

Received: October 23, 2024. **Revised:** February 19, 2025. **Accepted:** March 24, 2025

successful implantation and the development of the embryo in the endometrium. The endometrium is a dynamic tissue which undergoes tightly regulated, cyclic alterations. In the early secretory phase of the menstrual cycle, endometrial stromal cells undergo a process known as decidualization. This process is essential for establishing a receptive endometrium, which is necessary for successful embryo implantation and pregnancy maintenance. During decidualization, endometrial stromal cells proliferate and differentiate from fibroblast-like stromal cells into polygonal, epithelial-like cells [9]. This transition involves extensive morphological and molecular changes, including glycogen and lipids accumulation, cytoskeletal reorganization, changes in gene expression, and modulation of signaling pathways [10]. Dysregulation of this process is associated with infertility, recurrent pregnancy loss, and other reproductive pathologies [11].

The phosphatidylinositol 3-kinase (PI3K)/AKT signaling pathway plays a central role in regulating cell survival, proliferation, and differentiation across various tissues, including the endometrium [12]. AKT consists of three isoforms (AKT1, AKT2, and AKT3) encoded by separate genes. Although these isoforms share up to 80% homology, they have distinct physiological functions [13]. AKT1 is primarily involved in regulating cell growth and survival, AKT2 plays a role in glucose metabolism and insulin signaling, and AKT3 is implicated in neurological development and function [14–16]. Despite their functional preferences, these isoforms can have overlapping or unique roles, depending on the tissue type and cellular context.

Mice with individual AKT isoforms knockouts are viable, but each knockout leads to distinct metabolic and physiological alterations, which have been critical to our understanding of the specific roles of each isoform. Mice lacking AKT1 experience reduced cell survival, resulting in growth retardation, smaller organ sizes, and higher perinatal mortality [14, 17]. In contrast, the absence of AKT2 impairs insulin-stimulated glucose uptake in skeletal muscle, liver, and adipose tissues, causing insulin resistance and diabetes-like phenotypes [15]. Mice lacking AKT3 do not exhibit impaired glucose homeostasis nor reduced overall growth but are characterized by reduced brain size, attributed to smaller cell size and decreased cell number [16].

Single-knockout experiments provide valuable insights but do not fully capture the unique and redundant functions of each isoform. Double-knockout experiments further elucidated these roles. Mice lacking both AKT1 and AKT2 show severely compromised development of the skin, bone, and muscle, along with defective adipogenesis, leading to death shortly after birth [18]. The simultaneous knockout of AKT1 and AKT3 results in embryonic lethality around day 12 due to growth defects, abnormal cardiovascular and nervous systems development, and placental vascular defects [19]. Mice with both AKT2 and AKT3 deficiencies exhibit disrupted glucose metabolism, as well as reduced body, brain, and testicular weights, but remain otherwise viable and healthy [20]. It has also been demonstrated that heterozygous mice with one functional AKT1 allele ($AKT1^{+/-}$ $AKT2^{-/-}$ $AKT3^{-/-}$) survive and develop normally, underscoring the critical role of AKT1 in embryonic development and postnatal survival. However, the downstream phosphorylation of AKT targets and the overall metabolic health of these mice remain unknown. Furthermore, most landmark studies have predominantly used male mice in their experiments [17, 20], while little attention is given to the effect of AKT isoform knockout on fertility, cyclicity, or gynecologic physiology [14–16]. The severe growth deficiency and early postnatal lethality of $AKT1^{-/-}$ $AKT2^{-/-}$ mice [18], the embryonic lethality of the $AKT1^{-/-}$ $AKT3^{-/-}$ mice at days 11–12 [19], and the lethality of triple-knockout mice ($AKT1^{-/-}$ $AKT2^{-/-}$ $AKT3^{-/-}$) [20] have precluded the investigation of fertility parameters in these contexts.

To address the knowledge gap concerning the specific roles of AKT isoforms in decidualization and fertility, further experiments are necessary. Given the physiological limitations of systemic knockouts, we used isoform-specific knockouts of AKT1 and AKT2 using a PGR-Cre and AKT-flox system, allowing tissue-specific knockout mainly in the ovary and endometrium [21]. We combined these models with AKT3 systemic knockout mice, creating all possible combinations of AKT isoform-specific abrogation. This approach enables us to dissect the individual functions of each isoform in a physiological setting, providing unprecedented insights into their roles during decidualization, implantation, and early pregnancy.

Our initial investigation focused on macroscopic effects of AKT isoform abrogation on female fertility. We characterized litter size, estrous cyclicity, and endometrial gland development. Our findings showed that the knockout of AKT1 and AKT2, particularly in combination, significantly reduced the fertility of female mice [22]. Interestingly, the ovarian function was not affected with results showing normal ovarian physiology and sex hormone level. This reduced fertility may partly result from the decreased endometrial gland number observed in AKT1–2 KO mice, as well as disruptions of the estrous cycle, particularly the prolonged diestrus stage. Interestingly, while AKT3 phosphorylation increased on day 5 of rat pregnancy, it did not appear to be required for normal fertility in our current mouse model [23].

Built upon these results, we sought to further understand the histological and molecular mechanisms involved with each AKT isoforms. To this end, we induced pseudogestational and gestational states in our combinatorial tissue-specific AKT knockout mouse model to study phenotypical changes in decidualization, implantation, and uterine horn physiology. Generally, we found that AKT1–2 KO mice failed to decidualize during pseudogestation and had less implantation sites. Through a combination of histological analyses, immunohistochemistry, and Western blotting, we examined the localization, expression, and activation of AKT isoforms and their downstream targets in the uterus during artificial decidualization and early gestation. Our experiments showed that AKT3 is the main isoform active on days 4 and 8 of pseudopregnancy, with low total pAKT levels in its absence and high levels in AKT1–2 KO mice.

Material and methods

PGR-Cre mouse models

Mice were housed in groups of four per cage with ad libitum access to food and water on a standard soy protein–free diet (2020X Teklad Global Soy Protein-Free Extruded; Envigo). Temperature and lighting cycle were regulated in the animal facility with a 14-h light:10-h darkness cycle. All procedures were performed in accordance with the regulations of the Canadian Council on Animal Care and as underlined in the approved protocol from the Good Health and Animal Care Committee of the Université du Québec

à Trois-Rivières. As described previously, our PGR-Cre/AKT isoform-specific mouse model was generated following in-house crossing steps of four different genotypes [22]. $PGR^{cre/+}$ mice were obtained from Dr Franco DeMayo (Baylor College of Medicine) [21]. $AKT1^{flox/flox}$, $AKT2^{flox/flox}$, and $AKT3^{-/-}$ mice were obtained from Dr M. Birnbaum (University of Pennsylvania, USA) [15, 16, 24]. All mice had C57BL/6J genetic background and were backcrossed every 10 generations to prevent genetic drift. Genotyping was performed by PCR analysis using specific probes and DNA extracted from ear punches with the Phire Animal Tissue Direct PCR Kit (Thermo Fisher Scientific, MA, USA).

Artificial decidualization and implantation sites

Pseudopregnancy was induced by co-caging female rats with vasectomized males and confirmed by checking the vaginal plug.

Pseudopregnancy induction: The estrous cycle of 10–14-week-old female mice was monitored daily in the morning via vaginal smear. During proestrous, mice were mated overnight with a vasectomized male, which was confirmed the following morning by the presence of a vaginal plug (considered day 1 of pseudopregnancy). On day 4 (between 15:00 and 17:00), artificial decidualization was induced by injecting intraluminally 20 μL of sesame oil (S3547; Sigma-Aldrich, MO, USA) into the right uterine horn. The uninjected left horn served as the control. For Figure 5, uteri were collected on day 4, prior to artificial decidualization induction. On day 8 of pseudopregnancy, the uteri were collected, and decidualization was confirmed via histological examination. For implantation site experiments, female mice were mated overnight with a fertile male. Mating was confirmed by vaginal plug observation (considered day 1 of pregnancy). On day 6, mice were euthanized, and their uteri were collected to count the number of implantation sites. Individual implantation sites were isolated for further analysis.

Tissue collection

Female mice were euthanized in an induction chamber filled with 5% isoflurane and oxygen, followed by cervical dislocation. Whole uteri were either submerged in paraformaldehyde (PFA) for histological analysis or flash-frozen and stored at −80°C for Western blot analysis. For histology, uteri were fixed in 4% PFA overnight at 4°C with gentle agitation. The following day, the uteri were dehydrated through sequential baths of EtOH (70%, 95%, and 100%) and paraffin-embedded using baths of Neo-Clear and paraffin. Uteri were then molded into paraffin blocks and sectioned using a microtome.

Hematoxylin and eosin

Paraffin-embedded uteri were sectioned transversally at 6-μm thickness using a HistoCore AUTOCUT microtome (Leica Microsystems, Concord, ON, CAN), with four sections placed on positively charged microscope slides. Sections were then deparaffinized in successive Neo-Clear baths and rehydrated in decreasing EtOH concentrations (100%, 95%, and 70%) finishing in dH_2O. Tissues were then stained with hematoxylin (Harris hematoxylin, #HHS128; Sigma-Aldrich) and eosin (Eosin Y, HT110216; Sigma-Aldrich), covered with mounting medium (Permount, #SP15; Fisher Scientific, MA, USA) and a coverslip following manufacturer's instructions. Imaging was performed using an OPTIKA microscope (B290TB) with a 4× objective and a 32-MP camera or a 40× objective with a 5.1-MP ocular camera (C-B5; OPTIKA, BG, ITA).

Immunohistochemistry

Immunohistochemistry was performed using paraffin-embedded uteri sections (6-μm thick). Sections were deparaffinized in three xylene baths and rehydrated in decreasing EtOH baths (100%, 95%, and dH_2O). Antigen retrieval was conducted using a pressure cooker set at high for 15 min while slides were submerged in a sodium citrate solution (100 mM sodium citrate, 5% Tween 20, pH 6.0). Peroxidase activity was inhibited using a 3% hydrogen peroxide solution for 10 min, and nonspecific binding was blocked with 5% normal goat serum (#5425; Cell Signaling Technology, MA, USA) diluted in tris-buffered saline/Tween 20 for 1 h at room temperature. All following incubations were performed in a humidity chamber. Sections were incubated with primary antibodies diluted in blocking solution overnight at 4°C. The following day, sections were incubated for 30 min with 25 μL SignalStain Boost Detection Reagent (#8125; Cell Signaling Technology) followed by an incubation in SignalStain DAB Substrate Kit (#8059; Cell Signaling Technology) ranging from 1 to 10 min depending on the antibody. Sections were finally counterstained with hematoxylin and covered with mounting medium (Immu-Mount; Thermo Fisher Scientific) and a coverslip. The primary antibodies used from Cell Signaling Technology: IGFBP1 (#31025, 1:200), Progesterone Receptor A/B (#8757, 1:150), PTGS2 (COX2) (#12282, 1:300), AKT (#4691, 1:150), pAKT substrate (#9614, 1:500), FOXO1 (#2880, 1:100), NF-kappaB p65 (#8242, 1:200), and FOXA2 (#8186, 1:400). Estrogen receptor alpha (#sc-542, 1:1000) antibody was obtained from Santa Cruz Biotechnology and Leukemia Inhibitory Factor (LIF) (#PA5-115510, 1:100) from Thermo Fisher Scientific.

Western blot

Flash-frozen whole uteri were thawed and lysed in 50 μL of cold radioimmunoprecipitation assay buffer supplemented with protease and phosphatase inhibitors (cOmplete and PhosSTOP; Roche Applied Science, IN, USA). Physical cell lysis was achieved by cutting the uteri with sterile scissors, followed by 10 s of sonication and 10-min rest on ice. After centrifugation, the protein supernatant was recovered, and concentration was measured by colorimetry (#5000112, DC Protein Assay kit II; Bio-Rad, CA, USA). Each sample (30 μg of protein) was loaded into a 12% SDS-PAGE gel for migration and transferred to a nitrocellulose membrane. Membranes were blocked with 5% milk in phosphate buffered saline/0.05% Tween 20 for 1 h at room temperature followed by primary antibody probing overnight at 4°C under gentle agitation. HRP-linked secondary antibody (#7074, 1:3000; Cell Signaling Technology) was used for 1 h at room temperature. Protein detection was performed using SuperSignal West Femto (Thermo Fisher Scientific) in a dark room (Epi Chemi II, UVP BioImaging Systems) mounted with a cooled CCD camera (BioChemi cooled camera; UVP BioImaging Systems). Primary antibodies from Cell Signaling Technology: pAKT (#4060, 1:1000), AKT total (#4691, 1:1000), pGSK3B (#5558, 1:1000), GSK3B (#12456, 1:1000), pP70S6K (#9234, 1:1000), P70S6K (#9202, 1:1000), PAR-4 (#2328, 1:1000), BAD (#9292, 1:1000), COX2 (#12282, 1:1000), and FOXA2 (#8186, 1:1000). LIF antibody (#PA5-115510,

1:1000) was obtained from Thermo Fisher Scientific and anti-B-actin–peroxidase antibody (#A3854, 1:40,000) from Sigma-Aldrich.

Statistical analysis

One-way analysis of variance (ANOVA) followed by a Tukey post hoc test was used for the implantation sites data (minimum of $n = 5$ per group). The artificial decidualization success rate was calculated using a binominal test comparing each group to wild type (WT). Statistical significance was set at $p < 0.05$ where $^{*}p < 0.05$, $^{**}p < 0.01$, $^{***}p < 0.001$, and $^{****}p < 0.0001$. All statistical analyses were performed using GraphPad Prism software version 8.0.1 (GraphPad Software Inc., CA, USA).

Results

Induction of artificial decidualization on the PGR-Cre mouse model

In this study, we used an artificially induced decidualization mouse model to better understand the specific role of AKT isoforms during this process. A schematic representation of our protocol is presented. Briefly, oil injection mimics embryo apposition during the implantation window and uteri were collected 4 days later for analysis (Figure 1A) [25]. When harvested, decidualization was physiologically observed on the right, oil-injected uterine horn, which was larger, longer, and more vascularized when compared to contralateral horn serving as a control (Figure 1B). Decidualization was confirmed histologically using H&E staining, as the endometrial stromal cell underwent phenotypic changes, transitioning from fibroblast to epithelial-like secretory cells expressing IGFBP1 (Figure 1C). To evaluate the importance of AKT isoforms during decidualization in different genotypes, the process was artificially induced, and the success rate was measured (Figure 1D). The results showed that the combined knockout of AKT isoforms significantly reduced the success rate of artificial decidualization (Figure 1E). Specifically, the success rate was 5% for AKT1–2 KO ($p < 0.0001$), 28% for AKT2–3 KO ($p < 0.0001$), and 21% for AKT1–3 KO ($p < 0.0001$) compared to 75% in WT mice. Interestingly, the success rate in AKT1 KO was significantly reduced to 36% ($p < 0.0001$). On the other hand, the success rate for AKT3 KO was 95%, higher than in WT, though this difference was not statistically significant ($p < 0.0634$). These results suggest functional redundancy between AKT isoforms, especially between AKT1 and AKT2. The absence of AKT1 alone had the most significant impact on decidualization, highlighting its central role in the process.

Physiological impact of isoform-specific AKT KO on decidualization

To better understand the role of AKT isoforms during decidualization, we investigated the physiological impact of their absence in different genotypes using histological analysis. We first examined the macroscopic structure of the decidualized endometrium with transverse sections and H&E staining (Figure 2A). No clear differences were observed across the decidualized genotypes regarding vascularization and mesometrial and antimesometrial decidua structure. However, in AKT1–2 KO, artificial decidualization did not appear to occur. Higher magnification was used to examine the phenotype of decidualized endometrial stromal cells and the structure of endometrial glands, and to compare these parameters between genotypes (Figure 2B). Again, no difference was observed across genotypes except AKT1–2 KO, which was not further investigated due to its failure to decidualize. In general, decidualized endometrial stromal cells exhibited enlarged cytoplasm, rounded nucleus, and occasional multinucleation—hallmarks of decidualization. Finally, using immunohistochemistry, we analyzed the expression of key functional proteins during this process, such as ESR1, PGRA/B, PTGS2, and LIF (Figure 2C) and others (Supplementary Figure 1). Qualitative analysis of protein localization and expression in specific cell populations showed no significant difference between genotypes. While ESR1 signal slightly varies between genotypes, ESR1 and PGRA/B were primarily located in the nuclei of decidualized stromal cells, indicating their activity. PTGS2 was found in stromal cells near the epithelium, and LIF was extracellularly expressed in the antimesometrial decidua. These results suggest that the absence of specific AKT isoforms does not grossly affect the physiological aspects of artificial decidualization, except in AKT1–2 KO, where the process abrogated.

Expression and activation of AKT during decidualization

Since no overt physiological difference were observed, we further examined the expression and activity of AKT during decidualization in an isoform-specific manner. Using uterine transverse sections and immunohistochemistry, we first evaluated AKT expression across different uterine structures (Figure 3A). No differences were observed across genotypes, except in AKT1–2 KO where decidualization did not occur and was excluded from further experiments. Interestingly, the central antimesometrial decidua exhibited lower levels of AKT expression in all decidualized genotypes. At higher magnification, we evaluated AKT localization and expression in different cell populations, such as the epithelial, stromal, and endometrial gland cells (Figure 3B). AKT subcellular distribution remained consistent across genotypes. Lastly, we investigated AKT-dependent phosphorylation using an AKT motif-specific ($RXXS^{p}/T^{p}$) antibody to assess the impact of isoform-specific knockouts on AKT-dependent signaling (Figure 3C). No significant differences were observed in phosphorylation patterns among the genotypes. Overall, our results suggest that selective knockout of AKT isoforms does not affect the intracellular localization of remaining AKT isoforms or the broader phosphorylation patterns, indicating functional redundancy among AKT isoforms.

Localization, expression, and activation of AKT downstream targets during decidualization

The artificial decidualization success rates between AKT isoform KO models were notably different, though AKT isoform localization and expression did not seem grossly altered by their knockout counterparts. To understand the molecular basis of these functional differences, we further investigated downstream targets of AKT. Using immunohistochemistry, we evaluated the cellular localization of FOXO1 and NF-kappaB p65, two transcription factors partly regulated by AKT and essential for decidualization (Figure 4A–B). Both proteins showed similar subcellular localization across genotypes, with FOXO1 primarily in the nucleus and NF-kappaB

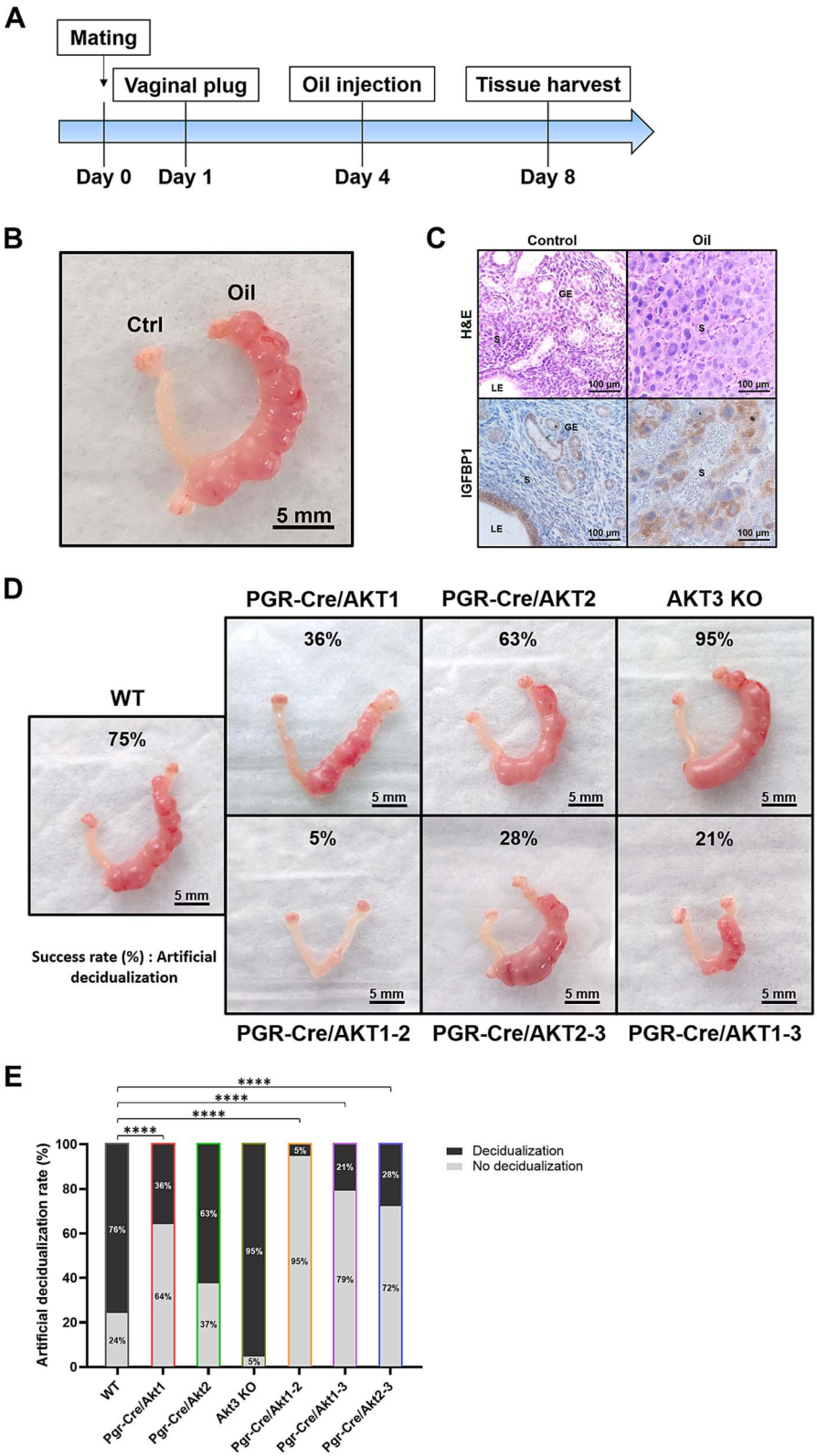

Figure 1. Induction of artificial decidualization in the PGR-Cre mouse model. (A) Schematic representation of the artificial decidualization protocol used in this study. (B) A representative uterus obtained from artificial decidualization induction. Female mice were mated with a vasectomized WT male. The uterus was harvested on day 8 of pseudopregnancy following sesame oil injection in the right uterine horn on day 4. The contralateral horn served as a control. Scale bar is 5 mm. (C) Validation of successful decidualization by physiology (H&E) and expression of a specific marker (IGFBP1). Paraffin-embedded control and oil-injected uteri from a WT mouse were sectioned transversally at a thickness of 6 μm. H&E staining was performed, and an IGFBP1 antibody was used to detect its expression by immunohistochemistry. Images were taken using a 40× microscope objective and a 5.1-MP camera. Scale bar represents 100 μm. GE, glandular epithelium; LE, luminal epithelium; S, stroma. (D) Representative decidualized uteri from each genotype. The percentage at the top of the image represents the success rate of artificial decidualization induction. Images were taken using a 32-MP camera. Scale bar is 5 mm. (E) The success rate of artificial decidualization induction was calculated for each genotype. Data were analyzed using a binomial test on GraphPad Prism 8 to compare each group to the expected rate from WT. A minimum of 18 independent experiments were performed ($n = 18$ mice/genotype). $^{****}p < 0.0001$. GE, glandular epithelium; LE, luminal epithelium; S, stroma.

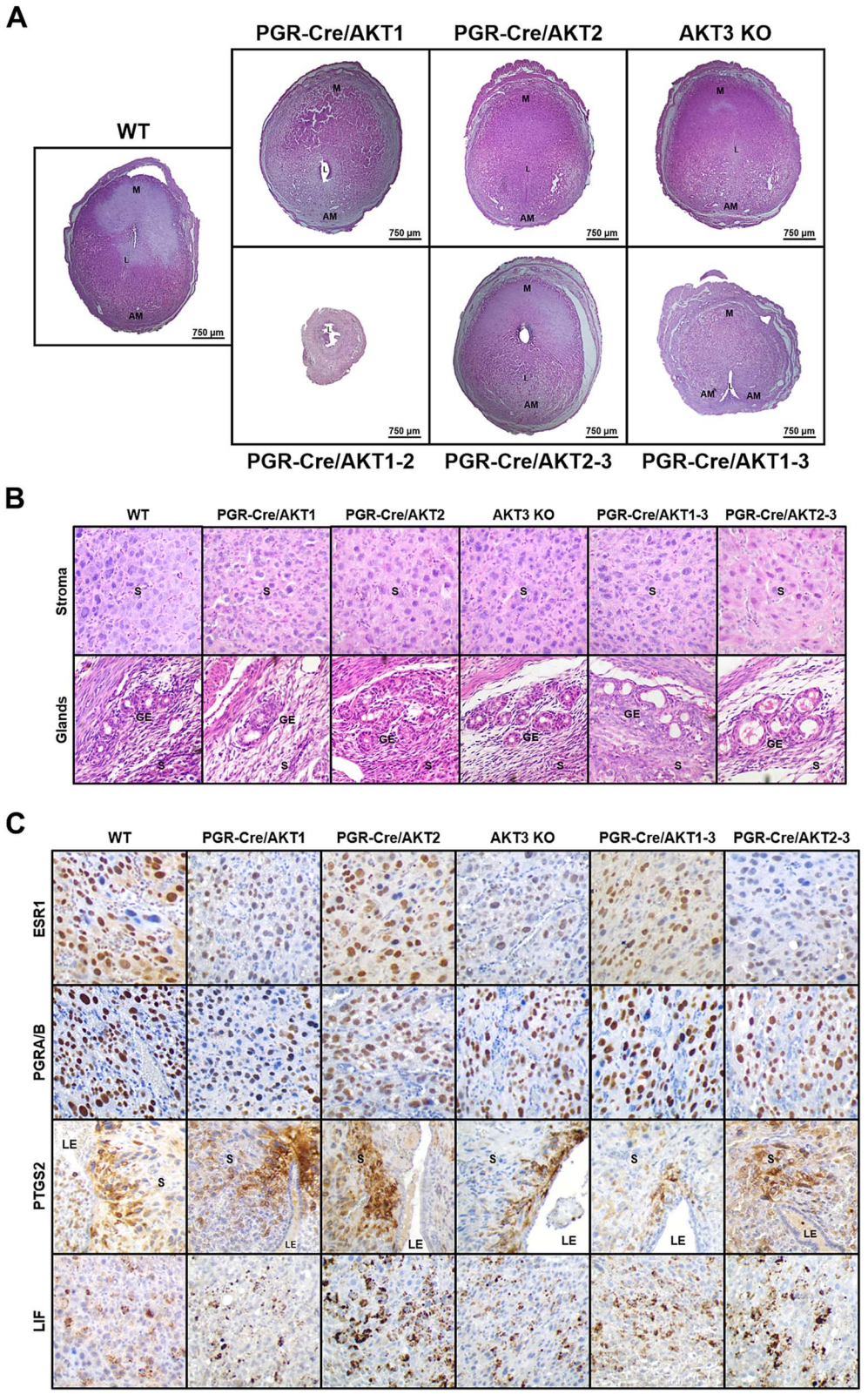

Figure 2. Physiological impact of isoform-specific AKT KO on decidualization. Female mice were mated with a vasectomized WT male, and the uterus was harvested on day 8 of pseudopregnancy following sesame oil injection in the right uterine horn on day 4. Paraffin-embedded decidualized uteri were sectioned transversally and stained using hematoxylin and eosin (H&E) or hematoxylin counterstained (IHC). (A) Representative H&E section of a decidualized uterus section from each genotype. Images were taken using a 4× microscope objective and a 32-MP camera. Scale bar represents 750 μm. M, mesometrial; AM, antimesometrial; L, lumina. (B) Representative H&E section of decidualized uteri showing stromal cells or endometrial glands from each genotype except PGR-Cre/AKT1–2. Images were taken using a 40× microscope objective and a 5.1 MP camera. (C) Using immunohistochemistry, the localization of ESR1, PGRA/B, PTGS2, and LIF protein expression was evaluated in each genotype of decidualized mice uteri except PGR-Cre/AKT1–2. GE, glandular epithelium; LE, luminal epithelium; S, stroma.

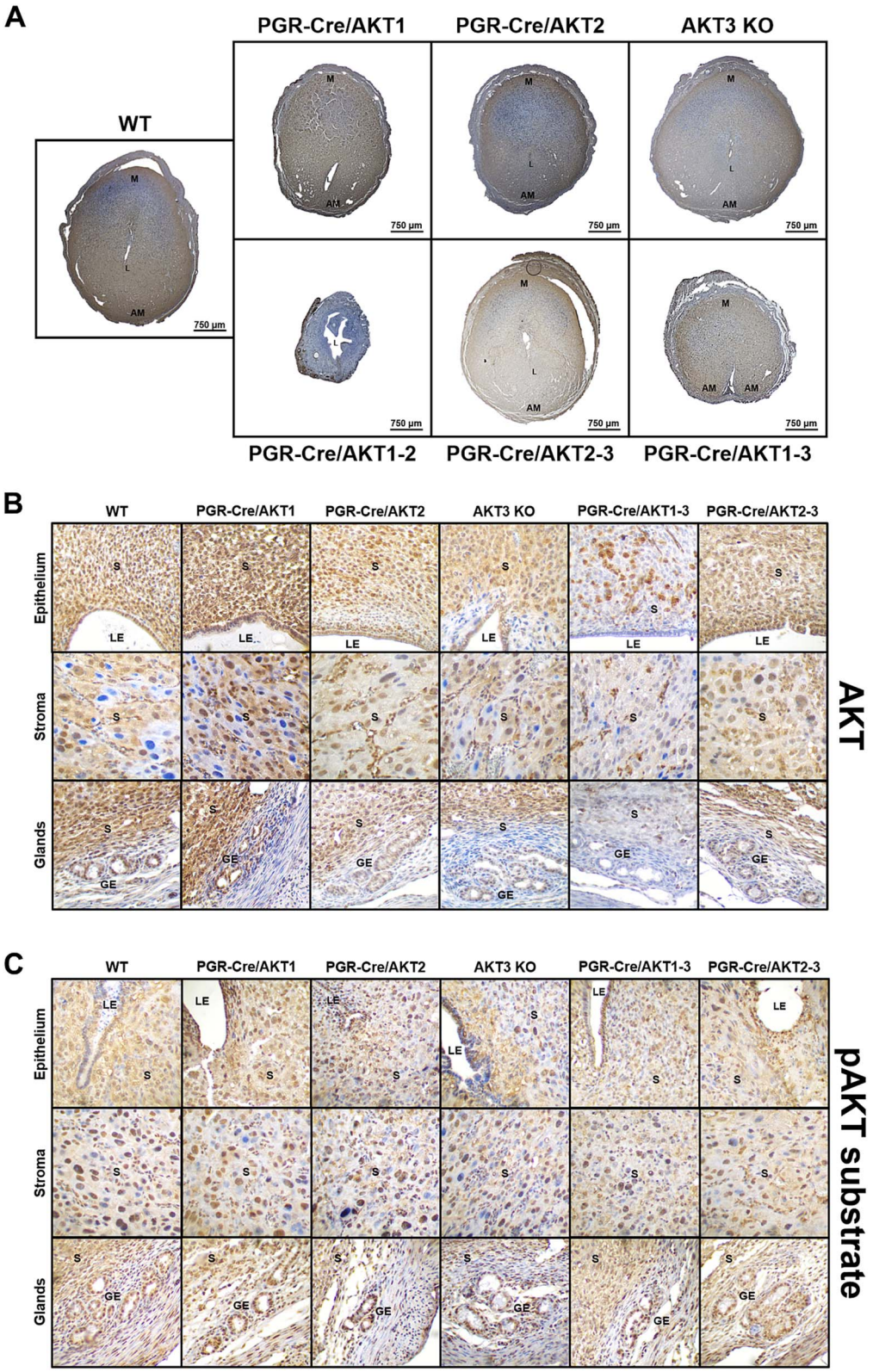

Figure 3. Expression and activation of AKT during decidualization. Female mice were mated with a vasectomized WT male and the uterus was harvested on day 8 of pseudopregnancy following sesame oil injection in the right uterine horn on day 4. (A) Paraffin-embedded decidualized uteri were sectioned transversally. AKT protein localization was evaluated in each genotype by IHC, with uteri counterstained with hematoxylin. Images were taken using a 4× microscope objective and a 32-MP camera. Scale bar is 750 μm. M, mesometrial; AM, antimesometrial; L, lumina. (B) Using the same decidualized slides, AKT localization in the epithelium, stroma, and endometrial glands was evaluated in each genotype except PGR-Cre/AKT1–2. Images were taken using a 40× microscope objective and a 5.1-MP camera. (C) Representative IHC of AKT activity level and localization (pAKT substrate antibody) using a decidualized uterus section counterstained with hematoxylin from each genotype except PGR-Cre/AKT1–2. Images were taken using a 40× microscope objective and a 5.1-MP camera. GE, glandular epithelium; LE, luminal epithelium; S, stroma.

p65 mostly in the cytoplasm. Next, we assessed isoform-specific AKT targets using Western blot (Figure 4C). Our results suggest that AKT3 is the main phosphorylated isoform during artificial decidualization, with reduced pAKT levels in AKT3 KO genotypes and increased level in AKT1–2 KO. AKT1–2 KO also showed increased levels of pGSK3B, PAR-4, BAD, FOXA2, and LIF, along with reduced expression of PTGS2 and phospho-P70S6K. These results suggest isoform-specific activity of AKT during decidualization, with reduced phosphorylation of AKT1 and AKT2 in this process. Concomitant abrogation of AKT1 and AKT2 signaling enhances AKT3 phosphorylation, indicating that pseudopregnancy favors AKT3 activation over AKT1 and AKT2.

Regulation of AKT activity on day 4 of pseudopregnancy

Since the success rate of artificial decidualization induction varied between genotypes, we investigated the regulation of AKT activity on day 4 of pseudopregnancy. The implantation window is crucial for inducing decidualization, so it is important to understand the variations observed in response to the oil stimuli in our experimental model. When the uteri were collected, we first assessed whether there were physiological differences across the genotypes (Figure 5A). Upon analysis, the uterine horns appeared similar, with only a slight increase in vascularization in preparation for implantation. We then examined proteins within the AKT signaling axis by evaluating their expression levels and activity using Western blot analysis (Figure 5B). Interestingly, our results suggest that AKT3 is the primary active isoform on day 4 of pseudopregnancy, with lower pAKT levels in its absence and higher levels in AKT1–2 KO mice. This variation in AKT activity seems to be associated with pGSK3B activity, as a similar pattern was observed, suggesting that pGSK3B may be AKT3 dependent. Another notable finding was the reduced expression of FOXA2 in AKT1–2 KO mice, accompanied by slightly lower levels of PTGS2, although no changes were observed in LIF protein levels. Taken together, our results suggest that AKT exhibits isoform-specific activity on day 4 of pseudogestation, influencing early decidualization. Interestingly, the phosphorylation of AKT1 and AKT2 was again reduced, more markedly than at day 8 of pseudogestation. The simultaneous abrogation of AKT1 and AKT2 signaling permits increased AKT3 phosphorylation and activation of downstream pathways. This regulatory mechanism is similar, yet distinct, from what we observed in late pseudopregnancy, suggesting that early pseudopregnancy almost completely inhibits AKT1 and AKT2 phosphorylation while favoring AKT3 activation and signaling.

Isoform-specific role of AKT in implantation sites

In our previous published study, AKT1–2 KO mice were subfertile, but no decidualization was observed during pseudopregnancy in our current experiments [22]. To better understand this outcome, we analyzed implantation sites in different genotypes during normal gestation, performing experiments to assess protein expression, activity, and localization. We collected uteri on day 6 of gestation to evaluate the physiological characteristics of the uterine horns and implantation sites (Figure 6A). Interestingly, we observed between 0 and 2 implantation sites in the AKT1–2 KO, always located near the proximal cervix. No significant physiological differences were observed in other genotypes. The number of implantation sites was also measured (Figure 6B). On average, WT female mice had nine implantation sites, which was consistent across other genotypes, except for AKT1–2 KO, which had an average of one implantation site ($p < 0.0001$). Next, we examined the protein levels of known regulators of implantation using Western blot (Figure 6C). In AKT1–2 KO mice, we observed slightly higher pAKT level and lower expression of FOXA2 and PTGS2, without affecting LIF protein levels. Since the sample were from whole tissue lysate, we performed immunohistochemistry on implantation sites to assess the expression and cellular localization of these proteins in endometrial stromal cells and glands (Figure 6D). Progesterone receptor expression and localization were similar across both cell populations in all three genotypes. AKT protein levels were lower in the stromal cells of AKT1–2 KO mice but similar in endometrial glands. Finally, LIF expression was lower in endometrial glands of AKT1–2 KO mice, despite similar expression levels in stromal cells. In conclusion, our results suggest that the absence of AKT1 and AKT2 significantly impacts the number of implantation sites during gestation on day 6, with lower expression of PTGS2 and LIF specifically in endometrial glands.

Discussion

In our present work, we have found that AKT1–2 KO mice fail to decidualize, explaining their subfertile phenotype. Notably, our results suggest that AKT3 is the main isoform active on day 4 of pseudopregnancy, with low total pAKT levels in its absence and high levels in AKT1–2 KO mice. Given that AKT3 KO mice were not previously found to be subfertile, this suggests that AKT3 activity is sufficient but not necessary for decidualization. This aligns with findings in human cell lines where overexpression of myr-AKT3 did not inhibit decidualization [26].

Our results also indicate that AKT1–2 phosphorylation is suppressed in early pseudopregnancy but gradually reinstated as time progresses. This corresponds with the fact that constitutive activation of AKT1–2 strongly impedes decidualization in human cells, blocking the initial response to second messenger and hormone-driven signaling [26]. Early pseudogestation may better represent the tissue's ability to decidualize, while late pseudogestation reflects other functions [27]. In this model, early pseudogestation requires the inhibition of AKT1–2 signaling, shifting the pathway toward AKT3. As time passes, AKT1–2 signaling is reinstated, though the mechanisms behind this remain unclear. At day 8 of pseudogestation, our results show that AKT1–2 knockout leads to dominant pAKT3 activity. Despite the increase in LIF, FOXA2, and pGSK3B in AKT1–2 KO mice, it seems unlikely that these are the specific downstream effectors whose reduced signaling causes decidualization failure. It should be noted that whether FOXA2 localization is changed in an isoform-specific manner remains to be determined. However, results at day 8 of pseudopregnancy show that pP70S6K is vastly reduced in AKT1–2 KO mice. In that context, it is plausible that AKT3, the singular, hyperphosphorylated isoform left, is unable to properly phosphorylate that target, thus failing to drive the AKT/MTOR axis.

Interestingly, our Western blot results show increased AKT3 activity in the absence of AKT1 and AKT2. This suggests that AKT3 is inhibited, either directly or indirectly, by the

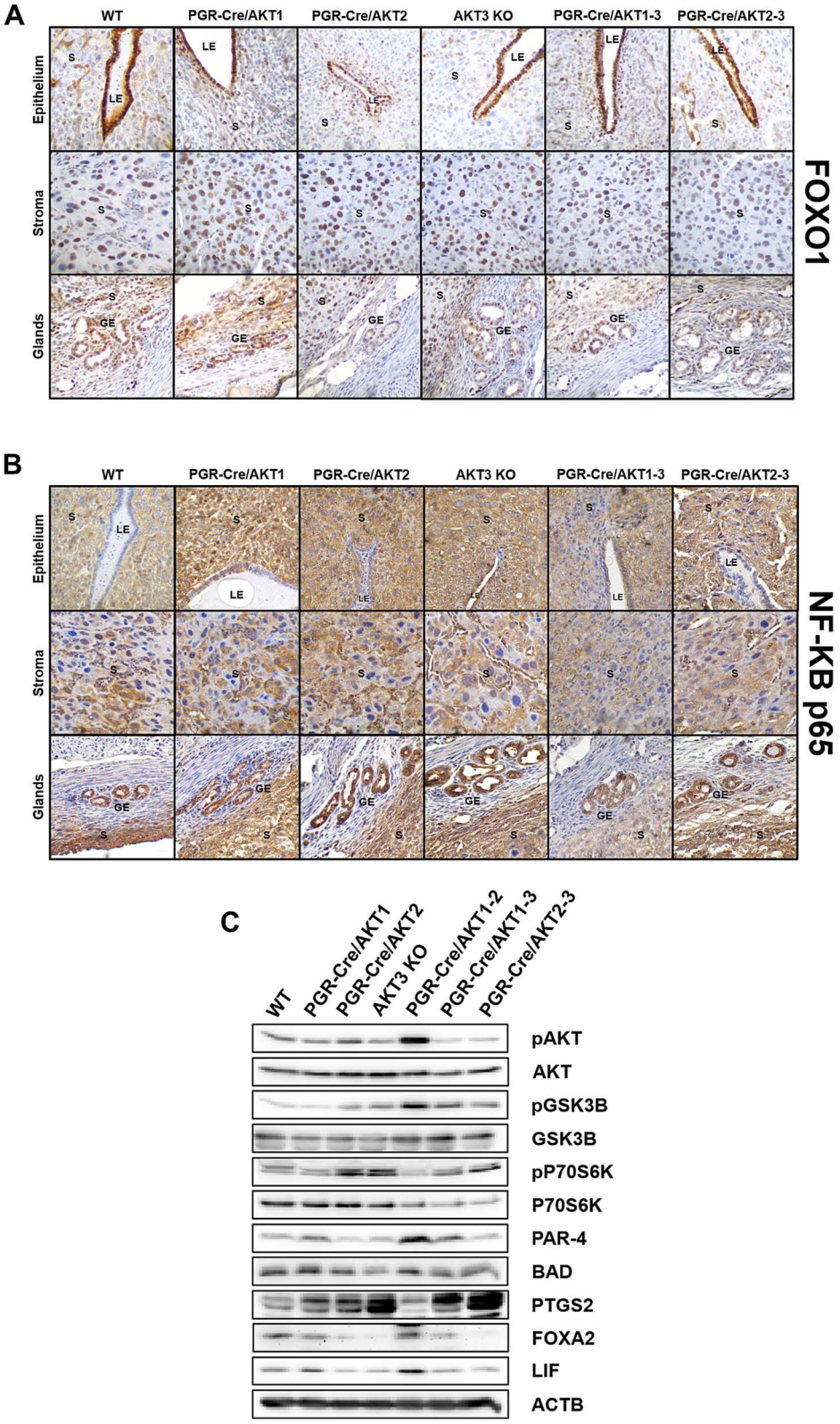

Figure 4. Localization, expression, and activation of AKT downstream targets during decidualization. Female mice were mated with a vasectomized WT male, and the uterus was harvested on day 8 of pseudopregnancy following sesame oil injection in the right uterine horn on day 4. Paraffin-embedded decidualized uteri were sectioned transversally. (A) Localization of FOXO1 and (B) NF-kappaB p65 proteins was evaluated in each genotype except PGR-Cre/AKT1–2 by IHC, with uteri counterstained with hematoxylin. Images were taken using a 40× microscope objective and a 5.1-MP camera. Scale bar is 750 μm. GE, glandular epithelium; LE, luminal epithelium; S, stroma. (C) Expression levels of different downstream targets of AKT were evaluated by Western blot for each genotype. Total proteins were isolated from whole decidualized uterus tissue. Beta-actin was used as a loading control, and the results shown are representative of four independent experiments ($n = 4$).

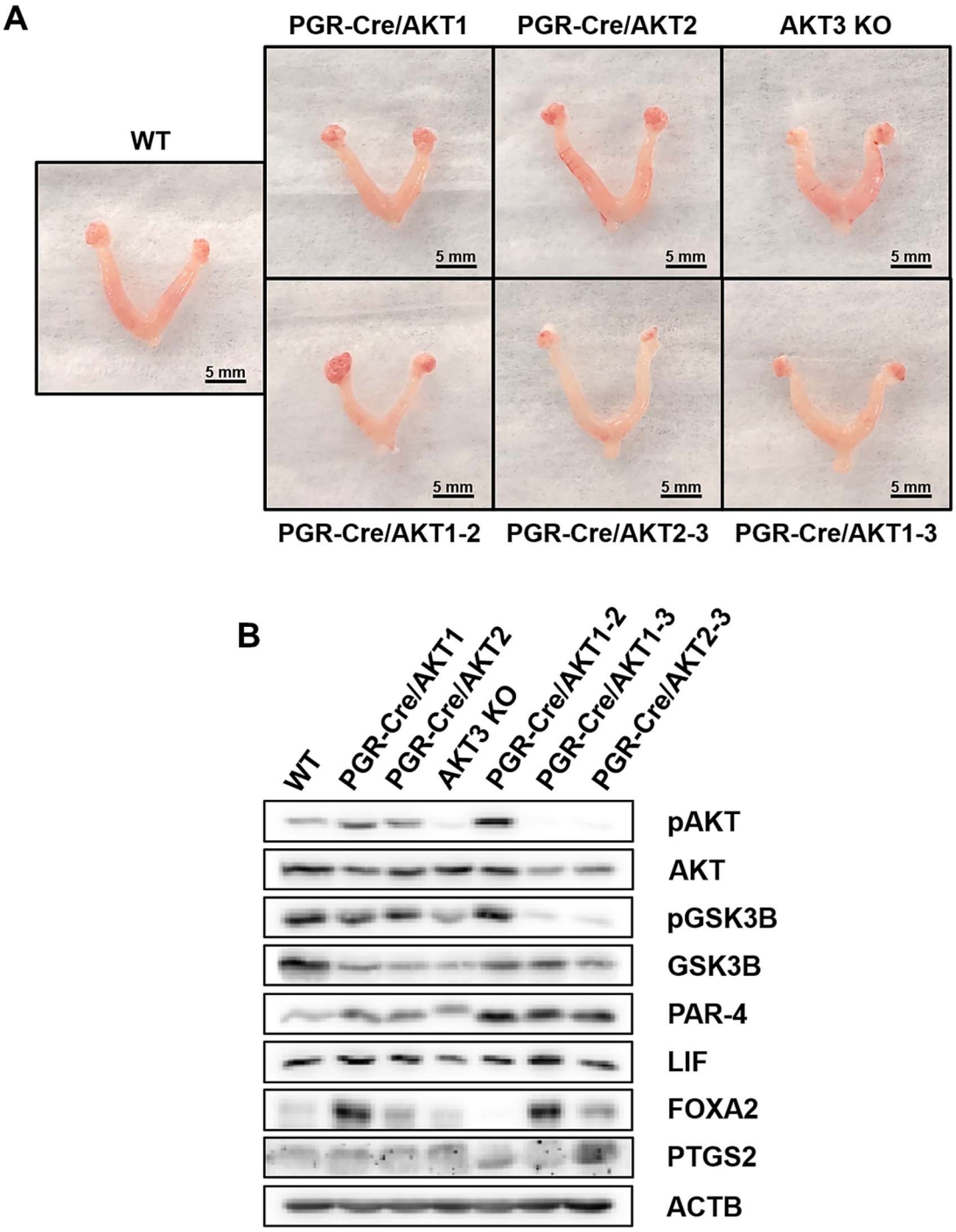

Figure 5. Regulation of AKT's activity on day 4 of pseudopregnancy. (A) A representative uterus obtained from inducing pseudopregnancy by mating a female mouse to a vasectomized WT male. The uterine horns were harvested on day 4 at the same time that the artificial decidualization induction surgery would occur. Scale bar is 5 mm. (B) Using Western blot, expression level of different downstream targets of AKT and endometrial gland function was evaluated for each genotype. Total proteins were isolated from whole uterus tissue at day 4 of pseudopregnancy. Beta-actin was used as a loading control, and the results shown are representative of five independent experiments ($n = 5$).

presence of its counterparts, and that the knockout of AKT1 and AKT2 removes this inhibition, allowing for increased AKT3 phosphorylation and its subsequent specific downstream signaling. Alternatively, it is possible that, due to the AKT1–2 KO, upstream mechanisms responsible for the phosphorylation of either of these kinases would drive the activation of AKT3 instead, given their structural similarities. Additionally, AKT1–2-specific downstream targets are likely involved in a negative feedback loop to mitigate AKT1–2 activity, a mechanism that would not be engaged by AKT3. The resulting effect of this bipartite pathway alteration would be the increased, aberrant, unchecked phosphorylation of AKT3. In this context, the upstream mechanisms responsible for the differential activation of all three AKT isoforms, as well as the putative mediators of that potential negative feedback loop, remain to be determined. Another consideration

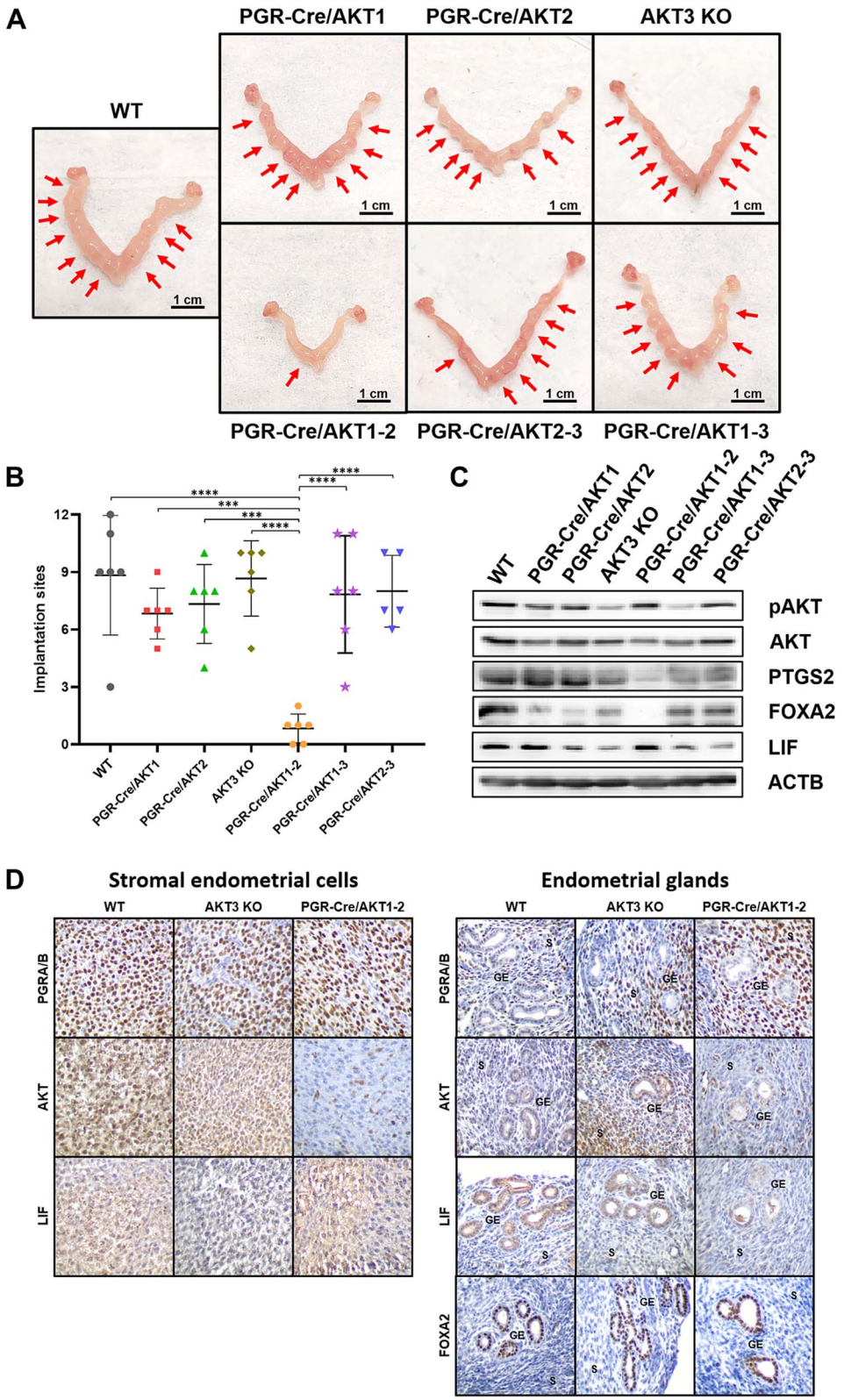

Figure 6. Isoform-specific role of AKT in implantation sites. (A) A representative uterus obtained from inducing gestation by mating a female mouse to a fertile WT male. The uterine horns were harvested on day 6 of gestation to count and collect implantation sites. An arrow indicates an implantation site. Scale bar is 1 cm. (B) Statistical analysis of the number of implantation sites at day 6 of gestation for each genotype. One-way ANOVA followed by Tukey post hoc test were performed on GraphPad Prism 8. All data are means ± SD of a minimum of five independent experiments ($n = 5$ mice/group). Individual dots represent a single mouse uterus implantation site count. ***$p < 0.001$; ****$p < 0.0001$. (C) Using Western blot, activation levels of AKT and protein expression of endometrial gland function were evaluated for each genotype. Total proteins were isolated from whole 2–3 implantation sites at day 6 of gestation. Beta-actin was used as a loading control, and the results shown are representative of four independent experiments ($n = 4$). (D) Paraffin-embedded uteri at day 6 of gestation were sectioned transversally from WT, AKT3 KO, and PGR-Cre/AKT1–2 genotypes. IHC was performed to evaluate PGRA/B, AKT, LIF, and FOXA protein expression and localization in stromal endometrial cells and glands. Uteri were counterstained with hematoxylin. Images were taken using a 40× microscope objective and a 5.1-MP camera.

is whether hyperactive AKT3 opposes decidualization and contribute to the subfertile phenotype of AKT1–2 KO mice or if the lack of AKT1–2 signaling is entirely responsible for this effect. Although these results have not reached statistical significance, AKT3 KO mice appear to be hyper-responsive to oil-induced decidualization. Moreover, our results suggest that AKT3 acts as a negative regulator of PTGS2 expression. It is possible that the lack of PTGS2, which is observed in AKT1–2 KO models, impairs decidualization. This could compound with the lack of downstream MTOR axis signaling found in that same genotype, as discussed previously. In this context, hyperactivation of AKT3, paired with the absence of AKT1–2 signaling, would explain the phenotype. Other proteins are likely a source of this differential AKT1–2-dependent regulatory network, with beta-catenin being a candidate for such isoform specificity in breast cancer [28]. In this context, AKT isoforms differentially downregulate beta-catenin levels and nuclear shuttling, an effect that again appears to be tissue specific. Moreover, beta-catenin gain-of-function mutations impede decidualization and embryo implantation through dysregulated crosstalk with stromal and epithelial cells. This could represent a potential mechanism by which AKT isoforms regulate endometrial receptivity and the sensitivity of decidualization triggers.

AKT3 presents the most structural and sequential differences compared to its counterparts, particularly in its linker domain [29]. This is consistent with its distinct involvement in various cellular processes, including tumorigenesis and tumor progression [30]. In the context of reproductive physiology, AKT1 and AKT2 activation seems to counteract decidualization in human cell models. Results suggest that their dephosphorylation, and subsequent inactivation, is essential for this process to occur. Interestingly, this is not the case for AKT3, as its overexpression and constitutive phosphorylation, via myristoylation, does not inhibit decidualization [26]. However, recent experiments using the same floxed mice models employed in the present study showed that while AKT3 is not essential for normal fertility in mice, AKT1 and AKT2 are [22]. These experiments affirm the existence of a fundamental functional overlap between AKT1 and AKT2, with a subset of shared functions crucial for fertility in mice. The experiments we conducted aimed to further elucidate this point and align our understanding with previous finding that overexpression of myr-AKT1 and myr-AKT2 inhibited decidualization in human cells [26]. The results presented here offer additional insight into this discrepancy.

It has been previously shown that decidualization requires cells to undergo mesenchymal to epithelial transition (MET), a process that opposes the canonical role of AKT, which is to drive epithelial-mesenchymal transition (EMT) [26]. This aligns with the initial loss of pAKT we observe in the presented experiments. Indeed, initial abrogation of this signaling axis could allow cells to further undergo MET, phenotypically progressing to the decidualized state. Additionally, AKT1–2 abrogation and solitary hyperphosphorylation of AKT3 appear to cause PAR-4 stabilization. We have previously shown that PAR-4 can drive TGFB1-induced EMT and is also directly involved in EMT induction [31]. However, this effect is likely tissue and cell type dependent and requires further investigation in healthy tissues, especially in the context of complex systems such as the live murine endometrium. Indeed, we have previously shown that decidualization provokes a marked nucleocytoplasmic shuttling of PAR-4, along with the concurrent nuclear entry of NF-kappaB [26]. Furthermore, this alteration in cellular protein partitioning was associated with the morphological changes linked to decidualization. Further experiments will be required to identify the effect of isoform-specific abrogation on PAR-4 intracellular localization and function. Indeed, PAR-4 has been shown to reduce AKT phosphorylation through PKCz in other cell models, an effect that appear at odds with the reported ability of AKT to directly bind and inactivate PAR-4 through phosphorylation [32]. This underlines the complex, reciprocal regulatory network in which PAR-4 is embedded, regulating multiple AKT-dependent axes while itself being regulated by the very same signaling pathways. It should also be noted that these experiments were performed with either AKT1 or without an isoform-specific approach, highlighting the potential isoform-distinct regulation of these mechanisms. Ultimately, there is a paucity of data surrounding the role of AKT in physiological mechanisms, and the interplay with specific AKT isoforms, independently of disease or physiological context, remains unelucidated.

One factor to consider is the method of inducing decidualization in mice using intraluminal sesame oil injection which is a key advantage since it allows the dissection of the isoform-specific role of AKT in an almost fully physiologic way. This artificial stimulus might elicit a more complex and nuanced response compared to direct induction via second messengers and hormones, as it is typically done in vitro. The oil-induced model likely triggers a broader, more intricate range of signaling pathways and cellular responses, distinct from the hormonally and cAMP-driven decidualization in vitro. This experimental condition complexifies the interpretation of murine results in comparison with human cell line models.

Mechanistic differences may also arise from the myristoylation of AKT isoforms, a model classically used in many in vitro experiments, which profoundly impacts intracellular signaling dynamics. Constitutive activation of myristoylated AKT1 and AKT2 forces them into membrane-bound signaling, while physiological signaling in murine models allows for unaltered intracellular localization and pan-cellular signaling of AKT isoforms. AKT isoforms likely demonstrate variable functions through substrate specificity, which arises not only from intrinsically differential substrate affinity but also from intracellular localization-dependent substrate availability [33]. This distinction between membrane-restricted and cellular-wide signaling may explain the observed differential effects but appears necessary to elucidate their unique as well as overlapping functions.

Moreover, living murine models presents additional complexity due to the simultaneous activation of multiple signaling pathways, sensitive to timing and cyclicity. In vitro systems lack the rhythmic fluctuations seen in vivo, where environmental inputs continuously modulate signaling pathways. Additionally, tissular microenvironments, characterized by the intricate interaction between multiple cell types, potentially regulate AKT isoform activity during pseudogestation, further contributing to the temporal shifts in AKT1 and AKT2 involvement in decidualization observed in the murine model.

While our experiments demonstrate minimal alterations in the subcellular localization of various proteins, it is important to acknowledge the inherent technical limitations of the methods employed. Immunohistochemistry, for instance, lacks the resolution necessary for highly granular analyses. Specifically, substrates like pAKT do not provide sufficient

clarity for precise organelle-level resolution. Although the general nuclear-cytoplasmic distribution remains consistent, this technique is inadequate for discerning finer localization shifts, such as AKT2's potential mitochondrial association or interactions with other organelles and proteins. Nevertheless, IHC proves sufficient for broad nuclear-cytoplasmic characterization, and within this scope, no significant changes were observed. Further experiments using high-resolution imaging methods could be performed to better characterize subcellular protein populations in key genotypes of interest.

The key question emerging from our results is as follows: if AKT1–2 oppose early pseudogestation and decidualization, and if AKT3 supports or at least does not impede this process, then why are AKT1–2 KO mice unresponsive to decidualization through oil injection? This question is pivotal, and our observations provide potential insights and avenues for further investigation. First, AKT1–2 KO mice are subfertile rather than infertile, with estradiol and progesterone levels comparable to WT mice. Despite normal hormone levels, these mice exhibit profound disruptions in estrus cycle rhythmicity and a marked reduction in gland number [22]. Additionally, while we can observe implantation sites, they appear to be anatomically restricted to the proximal cervix. Taken together, these findings suggests that AKT1–2 abrogation causes robust dysregulation of the uterine response to stimuli, whether hormonal or mechanical. This leads to altered glandular development, an abnormal estrous cycle rhythm, and resultant subfertility. It is also likely that the combined germinal uterine knockout of AKT1–2 causes underdevelopment of the uterus, further impeding its normal function and responsiveness.

Therefore, while AKT1–2 signaling may need to be dampened for decidualization to occur, the widespread uterine dysfunction found in AKT1–2 KO mice likely prevents decidualization in a pseudogestation model. This would be the case even in the presence of AKT3, which could otherwise act as a positive regulator of these early processes. To fully decipher the specific roles of AKT isoform in these mechanisms, it would be necessary to abrogate AKT1–2 expression in a temporally selective manner. Such a defined, pseudogestational stage-specific method would allow for normal organ development and the ability to stop AKT1–2 expression at various time points following pseudogestation inducement. This would provide a clearer understanding of each isoform's mechanistic contribution.

In conclusion, our results highlight the importance of AKT activity in the cellular and molecular regulation during mouse decidualization and embryo implantation. This study showed specific roles between each isoform, but also a partially redundant function of AKT1 and AKT2. AKT1–2 KO genotype failed to decidualize during pseudopregnancy and had a lower number of implantation sites while AKT3 was the main isoform active throughout decidualization. The PI3K/AKT pathway has an important role in fertility and a better understanding of the histological and molecular mechanisms involved with each AKT isoforms is necessary.

Acknowledgment

We are grateful to Dr Franco DeMayo (Baylor College of Medicine) and Dr M. Birnbaum (University of Pennsylvania) for the transgenic mice.

Conflict of interest: The authors have declared that no conflict of interest exists.

Data availability

All data are incorporated into the article and its online supplementary material.

Author contributions

PA, SP, and EA conceived and planned the experiments. PA carried out the experiments and analyzed the data. LIR performed some IHC. PA and FF wrote the manuscript. EA and MC reviewed the manuscript. EA and MC supervised the research project.

References

1. Vander Borght M, Wyns C. Fertility and infertility: definition and epidemiology. *Clin Biochem* 2018; **62**:2–10.
2. Bushnik T, Cook JL, Yuzpe AA, Tough S, Collins J. Estimating the prevalence of infertility in Canada. *Hum Reprod* 2012; **27**: 738–746.
3. Dayan N, Velez MP, Vigod S, Pudwell J, Djerboua M, Fell DB, Basso O, Nguyen TV, Joseph KS, Ray JG. Infertility treatment and postpartum mental illness: a population-based cohort study. *CMAJ Open* 2022; **10**:E430–E438.
4. Homan GF, Davies M, Norman R. The impact of lifestyle factors on reproductive performance in the general population and those undergoing infertility treatment: a review. *Hum Reprod Update* 2007; **13**:209–223.
5. Hruska KS, Furth PA, Seifer DB, Sharara FI, Flaws JA. Environmental factors in infertility. *Clin Obstet Gynecol* 2000; **43**:821–829.
6. Makar RS, Toth TL. The evaluation of infertility. *Am J Clin Pathol* 2002; **117**:S95–S103.
7. Idelevich A, Vilella F. Mother and embryo cross-communication. *Genes (Basel)* 2020; **11**:4.
8. Cha J, Sun X, Dey SK. Mechanisms of implantation: strategies for successful pregnancy. *Nat Med* 2012; **18**:1754–1767.
9. Gellersen B, Brosens IA, Brosens JJ. Decidualization of the human endometrium: mechanisms, functions, and clinical perspectives. In: *Seminars in Reproductive Medicine*, vol. **25**. © Thieme Medical Publishers, Imperial College London, Hammersmith Hospital, London, United Kingdom; 2007: 445–453.
10. Okada H, Tsuzuki T, Murata H. Decidualization of the human endometrium. *Reprod Med Biol* 2018; **17**:220–227.
11. Ng SW, Norwitz GA, Pavlicev M, Tilburgs T, Simón C, Norwitz ER. Endometrial decidualization: the primary driver of pregnancy health. *Int J Mol Sci* 2020; **21**:4092.
12. Fabi F, Asselin E. Expression, activation, and role of AKT isoforms in the uterus. *Reproduction* 2014; **148**:R85–R95.
13. Clark AR, Toker A. Signalling specificity in the Akt pathway in breast cancer. *Biochem Soc Trans* 2014; **42**:1349–1355.
14. Cho H, Thorvaldsen JL, Chu Q, Feng F, Birnbaum MJ. Akt1/PKBalpha is required for normal growth but dispensable for maintenance of glucose homeostasis in mice. *J Biol Chem* 2001; **276**:38349–38352.
15. Cho H, Mu J, Kim JK, Thorvaldsen JL, Chu Q, Crenshaw EB III, Kaestner KH, Bartolomei MS, Shulman GI, Birnbaum MJ. Insulin resistance and a diabetes mellitus-like syndrome in mice lacking the protein kinase Akt2 (PKBβ). *Science* 2001; **292**:1728–1731.
16. Easton RM, Cho H, Roovers K, Shineman DW, Mizrahi M, Forman MS, Lee VM, Szabolcs M, de Jong R, Oltersdorf T, Ludwig T, Efstratiadis A, *et al.* Role for Akt3/protein kinase Bγ in attainment of normal brain size. *Mol Cell Biol* 2005; **25**:1869–1878.
17. Chen WS, Xu PZ, Gottlob K, Chen ML, Sokol K, Shiyanova T, Roninson I, Weng W, Suzuki R, Tobe K, Kadowaki T, Hay N. Growth retardation and increased apoptosis in mice with homozygous disruption of the Akt1 gene. *Genes Dev* 2001; **15**: 2203–2208.
18. Peng XD, Xu PZ, Chen ML, Hahn-Windgassen A, Skeen J, Jacobs J, Sundararajan D, Chen WS, Crawford SE, Coleman KG, Hay N. Dwarfism, impaired skin development, skeletal muscle atrophy,

delayed bone development, and impeded adipogenesis in mice lacking Akt1 and Akt2. *Genes Dev* 2003; **17**:1352–1365.
19. Yang ZZ, Tschopp O, di-Poï N, Bruder E, Baudry A, Dümmler B, Wahli W, Hemmings BA. Dosage-dependent effects of Akt1/protein kinase Balpha (PKBalpha) and Akt3/PKBgamma on thymus, skin, and cardiovascular and nervous system development in mice. *Mol Cell Biol* 2005; **25**:10407–10418.
20. Dummler B, Tschopp O, Hynx D, Yang ZZ, Dirnhofer S, Hemmings BA. Life with a single isoform of Akt: mice lacking Akt2 and Akt3 are viable but display impaired glucose homeostasis and growth deficiencies. *Mol Cell Biol* 2006; **26**:8042–8051.
21. Soyal SM, Mukherjee A, Lee KYS, Li J, Li H, DeMayo FJ, Lydon JP. Cre-mediated recombination in cell lineages that express the progesterone receptor. *Genesis* 2005; **41**:58–66.
22. Adam P, Tardif L, Fabi F, Likonza Lokengo D, Renaud LI, Parent S, Cadrin M, Boerboom D, Asselin E. Redundant roles of AKT1 and AKT2 in fertility, estrous cyclicity and endometrial gland development. *Reproduction* 2023; **165**:605–616.
23. Veillette A, Grenier K, Brasseur K, Fréchette-Frigon G, Leblanc V, Parent S, Asselin E. Regulation of the PI3-K/Akt survival pathway in the rat endometrium. *Biol Reprod* 2013; **88**:79.
24. Wan M, Easton RM, Gleason CE, Monks BR, Ueki K, Kahn CR, Birnbaum MJ. Loss of Akt1 in mice increases energy expenditure and protects against diet-induced obesity. *Mol Cell Biol* 2012; **32**:96–106.
25. Finn C, Keen P. The induction of deciduomata in the rat. *Development* 1963; **11**:673–682.
26. Fabi F, Grenier K, Parent S, Adam P, Tardif L, Leblanc V, Asselin E. Regulation of the PI3K/Akt pathway during decidualization of endometrial stromal cells. *PLOS One* 2017; **12**:e0177387.
27. Ramathal CY, Bagchi I, Taylor R, Bagchi M. Endometrial decidualization: of mice and men. In: *Seminars in Reproductive Medicine*, vol. **28**. © Thieme Medical Publishers, University of Illinois at Urbana-Champaign, 524 Burrill Hall, 407 S. Goodwin Ave, Urbana, IL 61801; 2010: 017–026.
28. Hinz N, Jücker M. Distinct functions of AKT isoforms in breast cancer: a comprehensive review. *Cell Commun Signal* 2019; **17**:154.
29. Fortier AM, Asselin E, Cadrin M. Functional specificity of Akt isoforms in cancer progression. *Biomol Concepts* 2011; **2**:1–11.
30. Degan SE, Gelman IH. Emerging roles for AKT isoform preference in cancer progression pathways. *Mol Cancer Res* 2021; **19**:1251–1257.
31. Chaudhry P, Fabi F, Singh M, Parent S, Leblanc V, Asselin E. Prostate apoptosis response-4 mediates TGF-β-induced epithelial-to-mesenchymal transition. *Cell Death Dis* 2014; **5**:e1044.
32. Joshi J, Fernandez-Marcos PJ, Galvez A, Amanchy R, Linares JF, Duran A, Pathrose P, Leitges M, Cañamero M, Collado M, Salas C, Serrano M, *et al*. Par-4 inhibits Akt and suppresses Ras-induced lung tumorigenesis. *EMBO J* 2008; **27**:2181–2193.
33. Ebner M, Sinkovics B, Szczygieł M, Ribeiro DW, Yudushkin I. Localization of mTORC2 activity inside cells. *J Cell Biol* 2017; **216**:343–353.

Biology of Reproduction, 2025, 112(6), 1134–1147
https://doi.org/10.1093/biolre/ioaf062
Research Article